Comput Visual Sci 1: 179–182 (1998)

Computing and
Visualization in Science

Letter

Numerical solution of parabolic equations related to level set formulation of mean curvature flow

Angela Handlovičová[1], **Karol Mikula**[1], **Alessandro Sarti**[2]

[1] Slovak University of Technology, Department of Mathematics, Radlinského 11, 813 68 Bratislava, Slovakia
[2] DEIS, University of Bologna, Italy and LBNL, University of California, Berkeley, USA

Received: 22 April 1997 / Accepted: 27 February 1998

Communicated by: G. Wittum

Abstract. Numerical approximation of a nonlinear diffusion equation of mean curvature flow type is discussed. Computational results related to image processing are presented.

In this paper we are dealing with the numerical approximation for (Evans & Spruck type) regularization of the following nonlinear degenerate parabolic equation

$$u_t = g(|\nabla u|)|\nabla u|\nabla.(\frac{\nabla u}{|\nabla u|}) \qquad (0.1)$$

in a domain $\Omega \subset \mathbb{R}^N$, which is accompanied with homogeneous Neumann boundary conditions and with some initial condition. The aim is to use the equation (0.1) or, more precisely, its reasonable regularization, for image and shape analysis. Then, initial condition represents the processed image and the function u, the solution of (0.1), the result of *nonlinear (geometrical) scaling* ([1], [2], [14], [20]). This kind of application of equation (0.1) is based on the motion of image silhouettes by their mean curvature. Thus, the image geometrical features are strongly respected and (0.1) is a representative geometry driven diffusion model.

Provided $g(s) = 1$, (0.1) is called *level set equation*, which has been proposed by Osher & Sethian ([18],[21]) for computation of moving fronts in interfacial dynamics. It has been used by Evans & Spruck ([11]) for a definition of *generalized mean curvature flow* of hypersurfaces, too. The *level set equation* moves each level set (namely, level line in 2D and level surface in 3D) of u with the velocity proportional to its normal mean curvature field. Moreover, it yields the so called *morphological principle*; if u is a solution then, for any nondecreasing function φ, $\varphi(u)$ is a solution as well. This *contrast invariant* property has large significance in the theory of image processing ([1]). On the other hand, these ideas have been used in [3], where the model like (0.1) has been suggested for computational image and shape analysis.

Applying the *level set equation* to initial image yields the silhouettes smoothing. We document this phenomenon in Figs. 1–4. Solving numerically a regularization of (0.1) (see (0.2)–(0.4)) we try to obtain a realistic (smooth) shape of 3D object – left heart ventricle ([17]). We visualize the level surface which represents the boundary of the volume containing the blood in several discrete moments of cardiac cycle. On the left sides of the figures, the unfiltered isosurfaces are plotted. There are many nonrealistic fingers, incisions and peaks caused by aquisition. We can move such surface in the direction of its inside normal vector field with the velocity proportional to the mean curvature. The motions of convex and concave pieces are opposite due to the curvature sign, and the large fingers shrink faster due to curvature dependence of flow. Thus, locally in scale, we can obtain reasonable smoothing of the isosurface. The results of such image processing are plotted on right sides of Figs. 1–4.

On the other hand, the model (0.1) can be used successively for image selective smoothing with conserving of edge positions ([19], [5], [3], [12], [13], [4]). The Perona-Malik function $g(s)$ depending on $|\nabla u|$ – edge indicator ($g(s) \to 0$ for $s \to \infty$) is used to ”stop” the motion of the silhouette-edges. The regions bettween them are smoothed due to the diffusion process. Here, we present Fig. 5 where two chromozomes are extracted from an initial rather noisy 3D-image by image selective smoothing (0.1) with $g(s) = 1/(1 + s^2)$.

A 2D example is given in Fig. 6. The ancient coat-of-arms of Slovak town Modra is scanned from a book where neither the paper nor the colours were of a good quality (left). On the right, the scaled-smoothed version is presented.

There are several approaches to solve mean curvature flow problem, primarily related to free boundary problems with surface tension. Some of them deal with the so called ”Lagrangean approach” where the moving curve or surface itself is the main object of modelling and computing ([16], [15], [9], [10]). The ”Eulerian approach” of Osher & Sethian handles implicitly the mean curvature motion passing the problem to higher dimensional space and solving there the *level set equation*. What has been somewhat artificial in interfacial dynamics is very natural for image processing; we handle in one all geometrical information contained in image greylevel intensity function u, unknown in (0.1).

The *level set equation* itself is degenerate parabolic and complicated from the computational point of view. Its viscos-

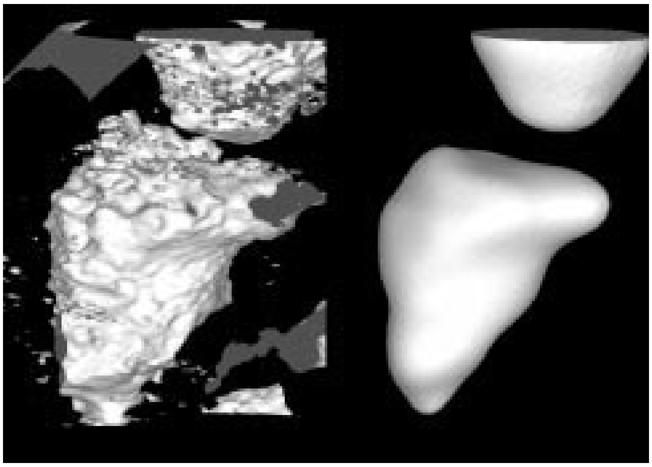

Fig. 1. The heart ventricle in systole phase – visualized from the result of aquizition *(left)* and after the 3D image processing by mean curvature flow *(right)*

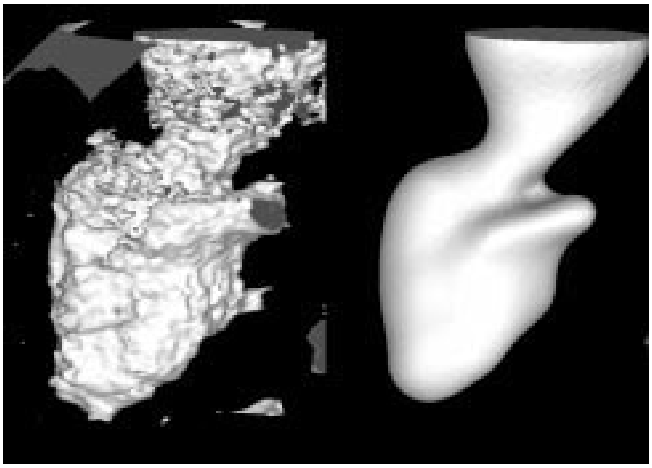

Fig. 2. The heart ventricle in open phase – visualized from the result of aquizition *(left)* and after the 3D image processing by mean curvature flow *(right)*

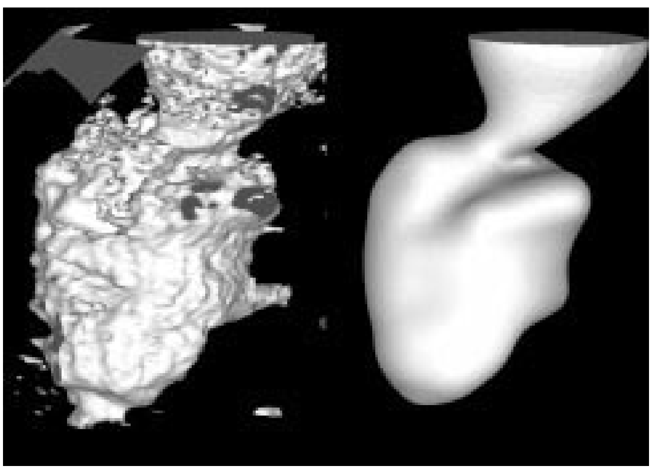

Fig. 3. The heart ventricle in open phase – visualized from the result of aquizition *(left)* and after the 3D image processing by mean curvature flow *(right)*

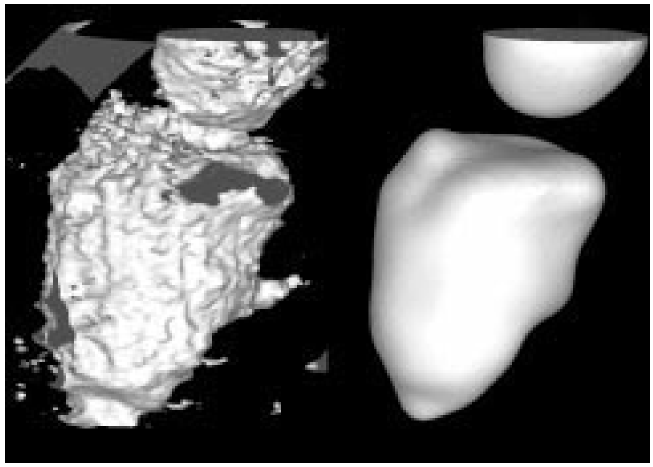

Fig. 4. The heart ventricle in diastole phase – visualized from the result of aquizition *(left)* and after the 3D image processing by mean curvature flow *(right)*

ity solution ([6], [7], [11]) can be tracked numerically e.g. by special techniques based on solution of Hamilton-Jacobi equations of first order ([18], [21]). We follow a totally different numerical approach. The motivation is to use standard numerical methods for solving parabolic PDEs, namely a finite element method for discretization in space and a kind of implicit method in scale. We solve a parabolic problem (in nondivergence form, however) which is close to the basic equation (0.1). For this purpose we use a special regularization depending on a small parameter ε used by Evans & Spruck in the proof of existence of a weak solution of *generalized mean curvature flow* ([11]). Their regularization is interpreted as a motion of a graph, with a slope proportional to $1/\varepsilon$, which is thus close to a cylinder with basis given by moving curve or surface. From [11], it is guaranteed that, for $\varepsilon \to 0$, solutions of the regularized problems tend to the viscosity solution of the *level set equation*.

We therefore solve numerically the following initial-boundary value problem

$$\frac{1}{\sqrt{\varepsilon + |\nabla u|^2}} u_t - g(|\nabla u|)\nabla.(\frac{\nabla u}{\sqrt{\varepsilon + |\nabla u|^2}}) = 0 \;\text{ in }\; I \times \Omega, \tag{0.2}$$

$$\partial_\nu u = 0 \;\text{ on }\; I \times \partial\Omega, \tag{0.3}$$

$$u(0,.) = u_0 \;\text{ in }\; \Omega, \tag{0.4}$$

where $1 > \varepsilon > 0$ is a (small) real number, $I = (0,T)$ is scale interval and $\Omega \subset \mathbb{R}^N$.

The semidiscrete version (Galerkin approximation) of (0.2) –(0.4) then reads as follows

$$\int_\Omega \frac{u_{h,t}\varphi_h}{g(|\nabla u_h|)\sqrt{\varepsilon + |\nabla u_h|^2}} + \int_\Omega \frac{\nabla u_h . \nabla \varphi_h}{\sqrt{\varepsilon + |\nabla u_h|^2}} = 0, \; \forall \varphi_h \in X_h, t \in I, \tag{0.5}$$

$$u_h(0,.) = \overline{u}_{h0}, \tag{0.6}$$

where $u_h(t,.) \in X_h$ is the approximation of u, X_h is space of linear finite elements with grid size parameter h and $\overline{u}_{h0}$ is the so called minimal surface projection of continuous initial data u_0 (see [8]).

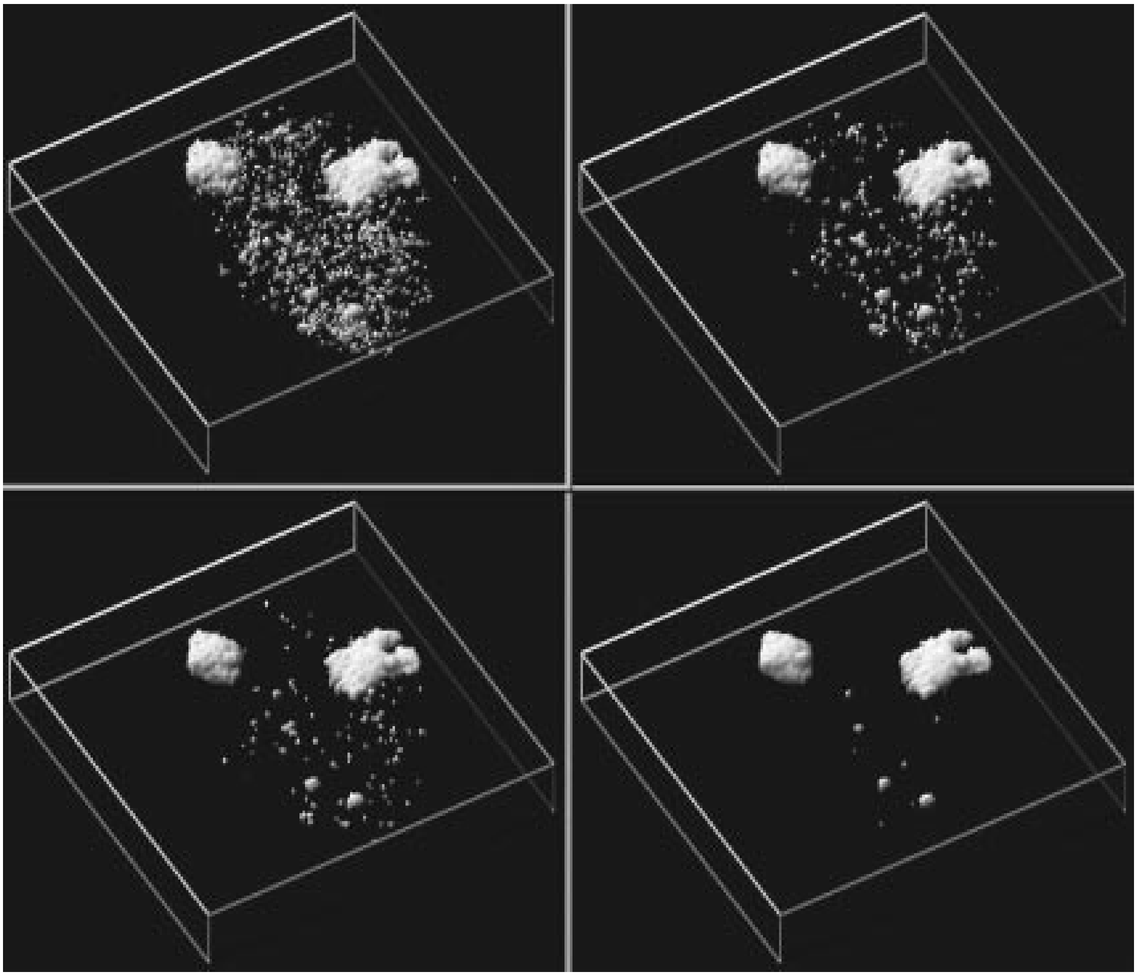

Fig. 5. Extraction of the chromozomes from the 3D image by mean curvature flow with velocity depending on the gradient of solution

In [8], the motion of two-dimensional nonparametric surface by its mean curvature, governed by equation

$$\frac{1}{\sqrt{1+|\nabla u|^2}} u_t - \nabla.(\frac{\nabla u}{\sqrt{1+|\nabla u|^2}}) = 0 \ \text{ in } I \times \Omega, \qquad (0.7)$$

is considered, provided $u = 0$ on $\partial\Omega, \Omega \subset \mathbb{R}^2$ and starting with smooth initial graph. For the fixed $\varepsilon > 0$, the structure of (0.2)–(0.4) differs only slightly from (0.7). Thus, in 2D case, one can use straightforwardly the ideas of Deckelnick and Dziuk to obtain the existence and uniqueness of the solution of the problems (0.2)–(0.4), (0.5)–(0.6), respectively, in proper functional spaces. Moreover the difference between u, solution of regularized problem (0.2)–(0.4), and u_h, solution of (0.5)–(0.6), depends on h in qualitatively same way as in [8] (Theorem 3.2). Thus the convergence of u_h to u in $L_\infty(I, L_2(\Omega)) \cap L_2(I, H^1(\Omega))$ is guarranteed for $h \to 0$.

In practical computations we solve (0.5)–(0.6) by a kind of semi-implicit method – treating the nonlinearities from the previous scale step. So, we choose discrete scale step τ and in each discrete scale moment $t_i = i\tau$ we solve

$$\int_\Omega \frac{(u_h^i - u_h^{i-1})\varphi_h}{g(|\nabla u_h^{i-1}|)\sqrt{\varepsilon + |\nabla u_h^{i-1}|^2}} + \tau \int_\Omega \frac{\nabla u_h^i . \nabla \varphi_h}{\sqrt{\varepsilon + |\nabla u_h^{i-1}|^2}} = 0, \quad \forall \varphi_h \in X_h$$

for the unknown function u_h^i. The convergence for such a full discrete scheme as well as the analysis of the limit behaviour $\varepsilon \to 0$ is an open question.

The computational grid is given naturally by the pixel (voxel) structure of the initial image. In experiments documented in Figs. 1–4 we used scale step $\tau = 10^{-4}$, regularization parameter $\varepsilon = 10^{-6}$ and we have computed 21 discrete scale steps. For the experiment from Fig. 5 we have choosen $\tau = 10^{-3}$, $\varepsilon = 10^{-6}$; the initial state and images after 6, 12 and 30 scale steps are plotted. In Fig. 6, the parameters are the same and we plot initial image and scaling version after 10 steps. In both cases we have $g(s) = 1/(1 + s^2)$.

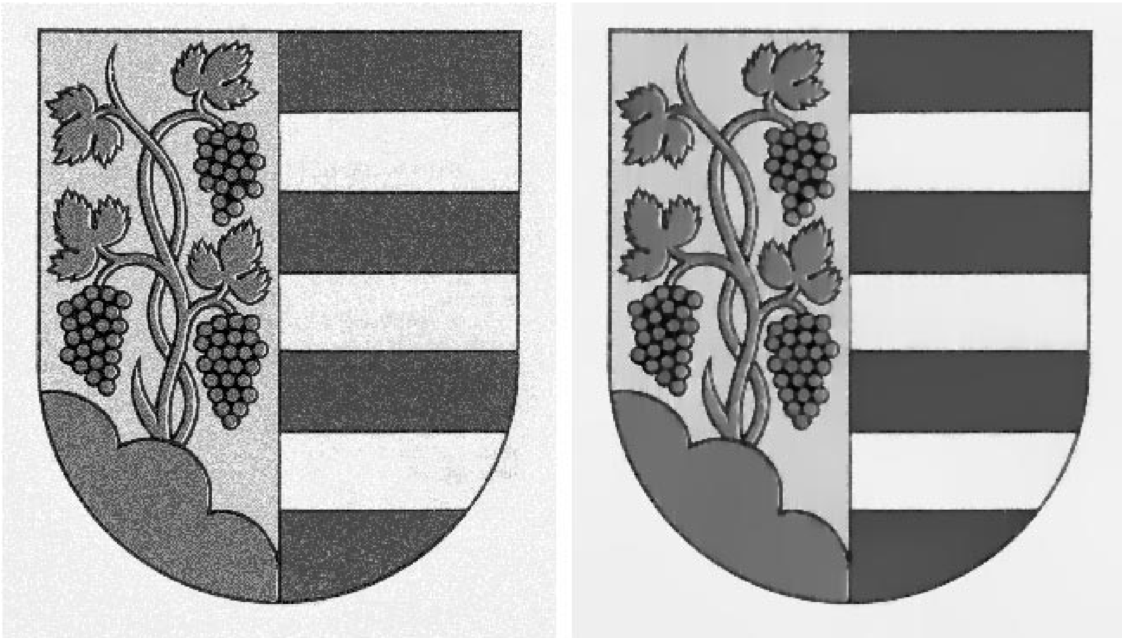

Fig. 6. Processing of the 2D image by mean curvature flow with velocity depending on the gradient of solution

Acknowledgement. We would like to thank to S. Cavalcanti and C. Lamberti from Bologna University and J. Wirth and R. Eils from IWR, University of Heidelberg for many fruitful disscussions, rendering of the testing data and the help in visualization. The numerical experiments presented in the paper were computed using large-scale computational facilities of CINECA – InterUniversity Computing Center, Bologna, Italy and IWR, University of Heidelberg, Germany. The computer resources and the visits of second author were supported by IPER ICARUS Project (funded by the European Commission – DGXII under the PECO program), Deutsche SFB 359 (Reactive Strömungen, Diffusion und Transport) and by the grants VEGA M63G, VEGA 1/3034/96 of the Slovak Republic. Last but not least we wish to thank to Professor W. Jäger for his support and interest in our work.

References

1. L.Alvarez, F.Guichard, P.L.Lions, J.M.Morel, Axioms and Fundamental Equations of Image Processing, Arch. Rat. Mech. Anal. **123** (1993), 200–257
2. L.Alvarez, J.M.Morel, Formalization and computational aspects of image analysis, Acta Numerica (1994), 1–59
3. L.Alvarez, P.L.Lions, J.M.Morel, Image selective smoothing and edge detection by nonlinear diffusion II, SIAM J. Numer. Anal. **29** (1992), 845–866
4. E.Bänsch, K.Mikula, A coarsening finite element strategy in image selective smoothing, Computing and Visualization in Science **1** (1997) 53–61
5. F.Catté, P.L.Lions, J.M.Morel, T.Coll, Image selective smoothing and edge detection by nonlinear diffusion SIAM J.Numer.Anal. **29** (1992), 182–193
6. Y.-G.Chen, Y. Giga, S. Goto, Uniqueness and existence of viscosity solutions of generalized mean curvature flow equation, J. Diff. Geom. **33** (1991), 749–786
7. M.G.Crandall, H.Ishii, P.L.Lions, User's guide to viscosity solutions of second order partial differential equations, Bull.(NS) Amer. Math. Soc. **27** (1992), 1–67
8. K.Deckelnick, G.Dziuk, Convergence of a finite element method for non-parametric mean curvature flow, Numer. Math. **72** (1995), 197–222
9. G.Dziuk, Convergence of a semidiscrete scheme for the curve shortening flow, Math. Models Methods Appl. Sci. **4** (1994), 589–606
10. G.Dziuk, Algorithm for evolutionary surfaces Numer. Math. **58** (1991), 603–611
11. L.C.Evans, J. Spruck, Motion of level sets by mean curvature I, J. Diff. Geom. **33** (1991), 635–681
12. J.Kačur, K.Mikula, Solution of nonlinear diffusion appearing in image smoothing and edge detection, Applied Numerical Mathematics **17** (1995), 47–59
13. J.Kačur, K.Mikula, Slow and fast diffusion effects in image processing-approximation schemes and numerical experiments, Preprint IWR 96-26, University of Heidelberg (1996)
14. P.L.Lions, Axiomatic derivation of image processing models, Math. Models Methods Appl. Sci. **4** (1994), 467–475
15. K.Mikula, Solution of curvature driven evolution of plane convex curves, Applied Numerical Mathematics **23** (1997) 347–360
16. K.Mikula, J.Kačur, Evolution of convex plane curves describing anisotropic motions of phase interfaces, SIAM J. Sci. Comput. **17** (1996), 1302–1327
17. K.Mikula, A.Sarti, C.Lamberti, Geometrical diffusion in 3D-echocardiography, Proceedings of ALGORITMY'97 – Conference on Scientific Computing, West Tatra Mountains – Zuberec (1997) 167–181
18. S. Osher, J. Sethian, Front propagating with curvature dependent speed: algorithms based on the Hamilton-Jacobi formulation, J. Comput Phys. **78**, 12–49
19. P.Perona, J.Malik, Scale space and edge detection using anisotropic diffusion, Proc. IEEE Computer Society Workshop on Computer Vision (1987)
20. B.M.ter Haar Romeny (Ed.), Geometry driven diffusion in computer vision, Kluwer (1994)
21. J. Sethian, Numerical algotithm for propagating interfaces: Hamilton-Jacobi equations and conservation laws, J. Diff. Geom. **31** (1990), 131–161